Sustainable Structures
ISSN: 2789-3111 (Print); ISSN: 2789-312X (Online)
http://www.sustain-dpl.com/journal/sust
DOI: 10.54113/j.sust.2025.000079

ORIGINAL ARTICLE

Improving the load-carrying capacity of structures consisting of multiple elements

Michael T. Todinov

School of Engineering, Computing and Mathematics, Oxford Brookes University
Oxford, OX3 0BP; UK, Email: mtodinov@brookes.ac.uk

Abstract: The paper presents a very powerful method in structural engineering, referred to as the method of aggregation, for reducing the weight and increasing load capacity of structures. Rigorous results have been stated and proved, forming the foundation of the aggregation method for structures composed of beams with arbitrarily shaped cross-sections. The essence of this method, overlooked in modern stress analysis, lies in consolidating loaded elements into a reduced number of elements with larger cross-sections, thereby significantly decreasing the material required to support a given total load. For instance, in a five-to-one aggregation of cantilever and simply supported beams, material usage can be reduced by a factor of 1.71. For cantilever and simply supported beams, the reduction in material volume, deflection, and stress depends only on the scaling factor of the cross-section along the *y*-axis and is independent of the scaling factor along the *x*-axis. The aggregation method was tested by a case study and finite element experiments involving structures built on statically determinate cantilever beams and statically indeterminate portal frames. These studies confirmed that aggregating elements loaded in bending leads to a drastic increase of the load capacity of the structures and a drastic decrease of both the maximum von Mises stress and the maximum deflection.

Keywords: Method of aggregation, light-weight design, load capacity, separation in geometry, structural optimization, cantilever beams, simply supported beams, frames, bending

1 Introduction

Separation in geometry has been used for a long time in design optimization as a foundational technique for reducing weight and enhancing the reliability and load capacity of components. It involves redistributing material and refining component shapes while adhering to specific load conditions, performance requirements, and constraints. Separation in geometry is a technique that is part of the domain-independent method of separation for improving reliability and reducing the risk of failure [1]. A common example of increasing the load capacity of components through separation in geometry is the tapered profile of a cantilevered beam, where thickness decreases from the fixed end toward the free end of the beam. For a given total volume of material, this tapered profile significantly enhances the load capacity. Another common example of increasing load capacity through separation in geometry is the adaptation in plates subjected to tension, where increasing material thickness around holes mitigates stress concentration, reduces peak stress and improves the plate's fatigue life.

Received: 24 November 2024; Received in revised form: 5 April 2025; Accepted: 8 May 2025

Topology optimization, developed as a mainstream design optimization technique for achieving lightweight structures, can also be regarded as a special case of the domain-independent approach "separation in geometry". In recent years, topology optimization has been widely applied to generate lightweight designs [2-4]. Several methods have been developed, including the evolutionary structural optimization method, the density method, and the level set method [2].

Advancements in manufacturing technologies, such as additive manufacturing (3D printing) [5,6,7] and advanced metal forming [8] helped produce component shapes that are difficult to produce using other methods. It also allows the integration of multiple functions into a single component, further improving load capacity at the same or reduced weight.

Aggregation of structural components made from different materials has also been exploited to obtain composite beams with superior flexural strength, exceeding the strength of the individual components. Examples include glass fiber and carbon fiber composite beams, beams made of steel-reinforced concrete, and sandwich beams. Sandwich beams, for example, utilize the principle of separation of functions in design: strong material located away from the neutral axis resists most of the load, while light and low-strength material near the neutral axis provides stability [9-11].

Aggregation techniques have been exploited in some structural designs where steel plates are aggregated by welding to form reinforced beams [12]. This increases the overall load-carrying capacity of the beam by allowing it to handle higher bending moments and shear forces. The structural performance of aggregated steel box beams filled with concrete has been investigated in [134].

In this paper, a different type of aggregation is discussed: the aggregation of identical structural components made of the same material into fewer identical structural components with larger cross-sections, under the same load.

The method of aggregation presented in this paper works for beams with arbitrary cross-sectional shapes, and the reduction in material needed to support the same specified total load is impressive. For example, in the case of five-to-one aggregation, the material usage can be reduced by a factor of 1.71. This makes the method of aggregation an extremely powerful tool in structural design optimisation for reducing weight and increasing load capacity.

For loaded components with arbitrarily shaped cross-sections, the method of aggregation has not yet been discussed with respect to optimizing the load capacity of structures. Multiple loaded elements are widely used in engineering and construction but in stress analysis literature, there is a lack of analysis regarding the effect of aggregation [10-11,14-18] of these elements, under the same total load. This is a striking omission considering the amount of research conducted in stress analysis.

Discussion related to the aggregation idea is also absent in structural engineering textbooks [19-21] and papers related to the optimization of loaded beams [22-23]. This critical discussion is also missing in the structural reliability literature [24-25]. The lack of discourse on the effects of aggregation of components with arbitrary cross sections therefore constitutes a significant knowledge gap, highlighting the need for further exploration.

We need to point out that although the proposed aggregation method is a kind of separation in geometry, it is a fundamentally different approach from the standard topology optimization approach and is developed without the help of any topology optimization algorithms. Topology optimization entails significant computational overhead due to the large number of iterative simulations required. In contrast, the proposed aggregation method does not involve any iterative simulations and incurs minimal computational overhead. Unlike topology optimization, the proposed method of aggregation is not affected by the size of the components composing the structures. Traditional manufacturing methods (casting, forging, machining) might not be suitable for intricate topologically optimized designs. Furthermore, designs obtained by topology optimization may have stress concentration points that cause premature fatigue failure.

None of these limitations exist for the aggregation method presented in the paper. Considering also the drastic weight saving achieved by this method, it is a valuable design optimization in structural engineering.

Bending, or flexural loading, is a very common type of loading. Elements with increased load capacity in bending are less likely to experience fatigue failure or premature failure due to overloading

or due to sudden application of loads. This results in a longer service life for the structure, reduced maintenance costs, and enhanced safety.

Consequently, through theoretical arguments and computer simulation experiments, the objectives of this study are:

(i) to provide the theoretical foundation of the aggregation method for design optimization of beams with arbitrarily shaped cross-sections;

(ii) to compare the amount of material required to support a specified total load for aggregated and non-aggregated structures with arbitrarily shaped cross-sections;

(iii) to compare the load capacities of aggregated and non-aggregated structures based on the same total volume of material;

(iv) to test the potential of the aggregation method on statically determinate and statically indeterminate components with arbitrary cross-sections;

The results of these studies are the main contributions of this paper and are directly related to structural design and reducing the risk of failure of structures loaded in bending.

2 A theoretical justification of the aggregation method for reducing the weight of structures

Consider a non-aggregated structure (**Fig.1a**) composed of n elements and an aggregated structure (**Fig.1b**) composed of a smaller number m of elements ($m < n$) with larger cross sections. Suppose that the cross sections of the aggregated structure are obtained from the cross sections of the non-aggregated structure by scaling along the x-axis and y-axis with factors $p_x \geq 1$ and $p_y \geq 1$. This means that any vector $\begin{bmatrix} x_0 \\ y_0 \end{bmatrix}$ from a non-aggregated cross section is transformed into the vector $\begin{bmatrix} x_a \\ y_a \end{bmatrix}$ from the aggregated section through the linear transformation

$$\begin{bmatrix} x_a \\ y_a \end{bmatrix} = \begin{bmatrix} p_x & 0 \\ 0 & p_y \end{bmatrix} \begin{bmatrix} x_0 \\ y_0 \end{bmatrix} = \begin{bmatrix} p_x x_0 \\ p_y y_0 \end{bmatrix} \tag{1}$$

where $\begin{bmatrix} p_x & 0 \\ 0 & p_y \end{bmatrix}$ is the scaling matrix defining the linear transformation. Because p_x and p_y are not necessarily equal, the non-aggregated and aggregated section are not necessarily geometrically similar. They will be geometrically similar only if $p_x = p_y = p$.

Let the non-aggregated structure be subjected to a total load P and the load per loaded element in the non-aggregated structure be P/n (**Fig.1a**). Similarly, let the aggregated structure be also subjected to a total load P and the load per element in the aggregated structure be P/m (**Fig.1b**). Let the maximum tensile stress permitted by the material be σ_{cr}. The key assumptions in deriving the next theoretical results are as follows:

- The beams cross-sections from the non-aggregated and aggregated structure are with arbitrary shape. The cross section of the aggregated structure is obtained through the scaling factors $p_x \geq 1$ and $p_y \geq 1$ along the x- and y-axis (see the example in **Fig.1c** and **1d**).
- For the sake of simplicity in presenting the relevant theory, a uniform cross section is assumed along the length of the beam.
- The material is homogeneous.
- The loading is uniformly distributed along the separate load-carrying elements.

These assumptions have been introduced to simplify the theory but do not necessarily limit the application of the aggregation method. As a general design approach, the aggregation method remains valid even if some of these assumptions are violated. For example, the method still works for structures with non-uniform sections along the length of the beam and for loads that are non-uniformly distributed along individual load-carrying elements.

Let σ_{cr} be the maximum permissible tensile stress for the material. To support the same total load *P* without exceeding the critical stress σ_{cr}, the corresponding total volumes of material for the non-aggregated and aggregated structure will be denoted by V_1 and V_2, correspondingly. An arbitrary cross-section of the non-aggregated beams has been assumed (**Fig.1c**). The maximum deflections of the non-aggregated and aggregated structures at the same total load *P*, will be denoted by δ_1 and δ_2, correspondingly. The length of the elements from the non-aggregated and aggregated structure is equal to *L*.

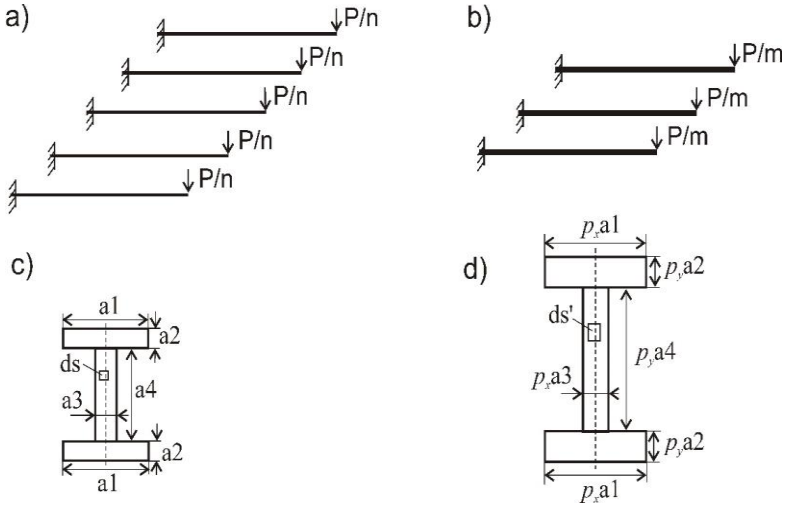

Fig.1 a) A non-aggregated structure built on *n* cantilever beams; b) An aggregated structure built on *m* cantilever beams (*m*<*n*); c) A beam cross section from the non-aggregated structure; d) A beam cross-section from the aggregated structure.

Theorem 1:

At the same maximum permissible tensile stress for a non-aggregated structure built on *n* identical cantilever or simply supported beams and an aggregated structure built on *m* identical cantilever or simply supported beams (*m*<*n*) with larger cross-sections, the following relationships hold:

$$V_1 / V_2 = p_y \tag{2}$$

$$\delta_1 / \delta_2 = p_y \tag{3}$$

where V_1, V_2 are the volumes of material needed to support a specified total load *P*, δ_1, δ_2 are the maximum deflections at the same total load *P*, and p_y is the scaling factor along the *y*-axis.

Proof:

Because of the scaling factors p_x and p_y, an elementary surface area $ds = \Delta x \Delta y$ in **Fig.1c** is transformed into the elementary area $ds' = p_x p_y \Delta x \Delta y$ in **Fig.1d**. As a result, between the cross-sectional area $S_1 = \iint dxdy$ of the elements from the non-aggregated structure and the cross-sectional area $S_2 = \iint dx'dy'$ of the elements from the aggregated structures, the following relationship exists:

$$S_2 = \iint dx'dy' = p_x p_y \iint dxdy = p_x p_y S_1 \tag{4}$$

For a bending moment *M* acting on a cantilever beam, the maximum tensile stress in the beam is determined from the classical formula:

$$\sigma = M\hat{y} / I \tag{5}$$

In equation (5), *I* denotes the second moment of area of the cross-section and $\hat{y}$ denotes the largest distance of a point from the cross section from the neutral axis. Because of the scaling factor p_y,

between the largest distance $\hat{y}_1$ characterizing the non-aggregated cross-section and the largest distance $\hat{y}_2$ characterizing the aggregated cross-section, the link:

$$\hat{y}_2 = p_y \hat{y}_1 \tag{6}$$

exists. The loading moment M_1 on a single element of the non-aggregated structure is $M_1 = (P/n)L$ while the loading moment M_2 on a single element of the aggregated structure is $M_2 = (P/m)L$. Now, following the definition of a second moment of area, let

$$I_1 = \iint y^2 dxdy \tag{7}$$

be the second moment of area of the non-aggregated sections (**Fig.1c**), where y is the distance of the infinitesimally small area $ds = dxdy$ from the neutral axis of the cross section. The second moment of area of the cross-section of an aggregated beam (see Fig.1d) is

$$I_2 = \iint y'^2 dx'dy' \tag{8}$$

where y' is the distance of the infinitesimally small area $ds' = dx'dy'$ from the neutral axis of the cross-section of the aggregated beam. Because of the proportionality factors $p_x \geq 1$ and $p_y \geq 1$, for the infinitesimally small dx' and dy', we have: $dx' = p_x dx$ and $dy' = p_y dy$. In addition, we have: $y' = p_y y$. The substitution in (8) then results in:

$$I_2 = p_y^3 p_x \iint y^2 dxdy = p_y^3 p_x I_1 \tag{9}$$

As a result,

$$I_2 / I_1 = p_y^3 p_x \tag{10}$$

of the aggregated and non-aggregated cross-sections.

For a critical tensile stress σ_{cr} and non-aggregated beam, equation (5) gives:

$$\sigma_{cr} = (P/n)L\hat{y}_1 / I_1 \tag{11}$$

while for an aggregated beam, equation (5) gives

$$\sigma_{cr} = (P/m)L\hat{y}_2 / I_2 \tag{12}$$

Taking the ratio of (11) and (12) results in

$$(m/n) \times \frac{I_2 \hat{y}_1}{I_1 \hat{y}_2} = 1 \tag{13}$$

Substituting (6) and (10) in (13) results in

$$(m/n) \times p_y^2 p_x = 1 \tag{14}$$

from which:

$$n/m = p_y^2 p_x \tag{15}$$

The total volume of the non-aggregated structure is $V_1 = nS_1 L$ while the total volume of the aggregated structure is $V_2 = mS_2 L$, where S_1 and S_2 are the cross sections of the non-aggregated and aggregated beams, correspondingly. Considering (4), we have

$$\frac{V_1}{V_2} = \frac{nS_1 L}{mS_2 L} = \frac{n}{m} \times \frac{1}{p_x p_y} \tag{16}$$

Substituting (15) in (16) finally gives:

$$\frac{V_1}{V_2} = \frac{p_x p_y^2}{p_x p_y} = p_y \tag{17}$$

This completes the proof of assertion (2) of Theorem 1, which is a new result in stress analysis. Equation (17) states that the volume reduction from aggregation depends on the scaling factor p_y along the *y*-axis and is independent of the scaling factor p_x along the *x*-axis. This means that if the scaling factor along the *y*-axis is $p_y = 1$, then $V_1 / V_2 = 1$ and although $p_x > 1$, the aggregation into fewer load-carrying elements with larger cross sections will not entail any material reduction.

For *n*-to-one aggregation (*m*=1), and $p_x = p_y$, from equations (15) and (17), it follows that

$$\frac{V_1}{V_2} = p_y = n^{1/3} \tag{18}$$

Fig. 2 presents the volume of material reduction factors for *n*=2, 3, 4 and 5.

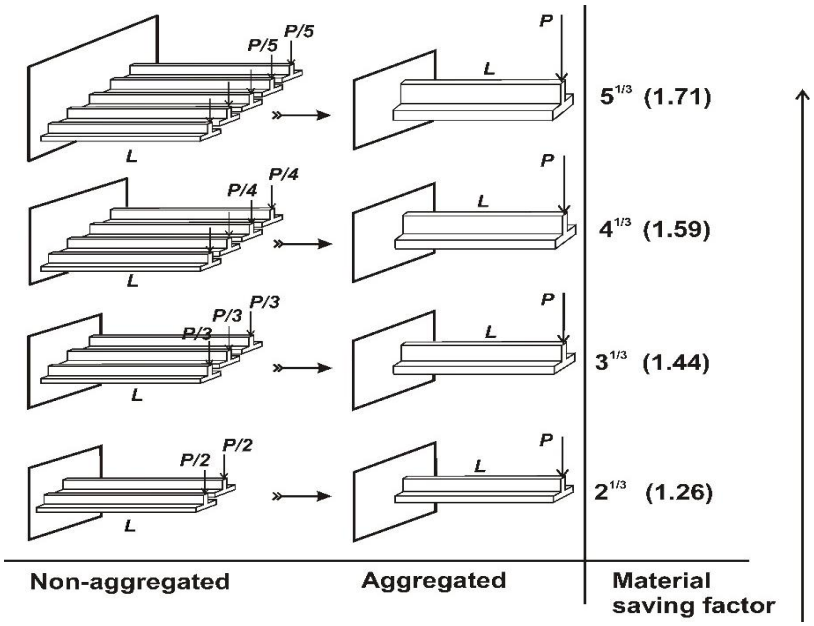

Fig.2. Material reduction factor for *n*-to-1 aggregation (n=2, 3, 4 and 5). The aggregated and non-aggregated structures carry the same total load *P*.

As can be seen from **Fig.2**, the reduction of material needed to support the same specified total load is impressive. For five-to-one aggregation, for example, the reduction in material used is 1.71 times!

From the classical stress analysis theory [12, 15], for the deflection at the free end of the non-aggregated cantilever beams, the value

$$\delta_1 = \frac{(P/n)L^3}{3EI_1} \tag{19}$$

is obtained and for the deflection at the free end of the aggregated cantilever beam, the value

$$\delta_2 = \frac{(P/m)L^3}{3EI_2} \tag{20}$$

is obtained, where *E* is the Young's modulus of the material of the beams.

Now, from expression (10), for the second moments of area of the aggregated cross-sections, the expression

$$I_2 = I_1 p_y^3 p_x \tag{21}$$

is obtained:

The ratio of the maximum deflections in the non-aggregated and aggregated structure is obtained by dividing equations (19) and (20):

$$\frac{\delta_1}{\delta_2}=\frac{(1/n)/I_1}{(1/m)/(p_y^3 p_x I_1)}=(m/n)p_y^3 p_x=\frac{p_y^3 p_x}{p_y^2 p_x}=p_y \tag{22}$$

This completes the proof of assertion (3) in Theorem 1.

Equation (22) means that the reduction in deflection depends on the scaling factor p_y along the *y*-axis and is independent of the scaling factor p_x along the *x*-axis. This means that if the scaling factor along the y-axis is $p_y=1$, then $\delta_1/\delta_2=1$ and although $p_x>1$, the aggregation into fewer load-carrying elements with larger cross sections will not entail any reduction of the maximum deflection.

The same analysis and the same results (17) and (22) are also obtained for simply supported beams and to conserve space, details related to the proof have been omitted.

A case study on cantilever beams illustrating the theory presented in this section has been presented in the Appendix.

3. Improving the load-bearing capacity at a constant amount of material

Suppose that the non-aggregated structure in **Fig.1a** includes *n* identical beams with arbitrary shape of the cross section while the aggregated structure in Fig.1b includes fewer number *m* of identical beams ($m < n$).

The beams from the non-aggregated and aggregated structure have cross sections with coefficients of proportionality $p_x \geq 1$ and $p_y \geq 1$ between the linear parameters (see the example in **Fig.1c** and **1d**). The coefficients of proportionality p_x, p_y, have now been selected such that the total volume of the non-aggregated structure is equal to the total volume of the aggregated structure.

Let $\sigma_{t,1}, \sigma_{t,2}$ denote the maximum tensile stress in the non-aggregated and aggregated structure correspondingly, while δ_1, δ_2 denote the maximum deflections of the non-aggregated and aggregated structure. The length of the beams from the non-aggregated and aggregated structure is equal to *L* and the total load for the non-aggregated and aggregated structure is equal to *P*.

Theorem 2:

The following relationships exist between the maximum tensile stresses $\sigma_{t,1}, \sigma_{t,2}$ and deflections δ_1, δ_2 of a non-aggregated structure built on *n* identical beams and an aggregated structure built on *m* identical beams ($m < n$), (the total volume of material and the total load are the same):

$$\sigma_{t,1}/\sigma_{t,2}=p_y \tag{23}$$

$$\delta_1/\delta_2=p_y^2 \tag{24}$$

Proof:

Because of the scaling factors p_x and p_y, an elementary surface area $ds=\Delta x\Delta y$ in **Fig.1c** is transformed into the area $ds'=p_x p_y \Delta x\Delta y$ in Fig.1d. The elementary volume $L\Delta x\Delta y$ from the non-aggregated structure is transformed into the elementary volume $Lp_x p_y \Delta x\Delta y$ from the aggregated structure. The total volume of the non-aggregated and aggregated structure must be the same, which yields the condition:

$$n\times\iint L dxdy = m\times p_x p_y \iint L dxdy \tag{25}$$

After cancelling $\iint L dxdy$ in (25), a condition is obtained for the scaling factors p_x, p_y which guarantee the equivalence of volumes of the non-aggregated and aggregated structure:

$$n/m = p_x p_y \tag{26}$$

Equation (26) shows that for equal total volumes of the aggregated and non-aggregated structure, for given *n* and *m*, the proportionality factors p_x and p_y, determining the cross-section of the aggregated elements cannot be chosen randomly. They must be selected such that relationship (26) holds.

From the classical bending theory, for the tensile stress at the fixed support of a non-aggregated cantilever beam, the value:

$$\sigma_{t,1} = (P/n)L\hat{y}_1 / I_1 \tag{27}$$

is obtained while for the aggregated beam, the value

$$\sigma_{t,2} = (P/m)L\hat{y}_2 / I_2 \tag{28}$$

is obtained, where $\hat{y}_1$ and $\hat{y}_2$ are the largest distances from the neutral axis for the non-aggregated and aggregated cross-section, correspondingly.

Because of the scaling factor p_y, for the largest distances from the neutral axis $\hat{y}_1$ and $\hat{y}_2$, the relationship

$$\hat{y}_2 = p_y \hat{y}_1 \tag{29}$$

holds. From equation (10), $I_2 / I_1 = p_y^3 p_x$. The ratio of the maximum tensile stresses in the non-aggregated and aggregated structure can then be obtained by dividing equations (27) and (28):

$$\frac{\sigma_{t,1}}{\sigma_{t,2}} = \frac{(1/n)\hat{y}_1 / I_1}{(1/m)p_y\hat{y}_1 / (I_1 p_y^3 p_x)} = \frac{(m/n)p_y^3 p_x}{p_y} = \frac{p_y^3 p_x}{p_x p_y^2} = p_y \tag{30}$$

For the maximum deflection of the non-aggregated cantilever beams, the value

$$\delta_1 = \frac{(P/n)L^3}{3EI_1} \tag{31}$$

is obtained from the standard bending theory [11,17] and for the maximum deflection of the aggregated cantilever beam, the value

$$\delta_2 = \frac{(P/m)L^3}{3EI_2} \tag{32}$$

is obtained, where *E* is the Young's modulus of the material of the beams.

The ratio of the maximum deflections in the non-aggregated and aggregated structure is obtained by dividing equations (31) and (32) and taking into consideration equation (26):

$$\frac{\delta_1}{\delta_2} = \frac{(1/n)/I_1}{(1/m)/(I_1 p_x p_y^3)} = (m/n)p_x p_y^3 = \frac{p_x p_y^3}{p_x p_y} = p_y^2 \tag{33}$$

This completes the proof of assertions (23) and (24) of Theorem 2 which are new results in stress analysis. Since $p_y > 1$, aggregation under the same total volume of material resulted in a smaller maximum tensile stress ($\sigma_{t,2} < \sigma_{t,1}$) and smaller deflection ($\delta_2 < \delta_1$). Another advantage of the aggregated structure over the non-aggregated one is the smaller number of connection points (anchors) during assembly. The same analysis and the same results (30) and (33) are also obtained for simply supported beams and to conserve space, details related to the proof have been omitted.

Assertions (23) and (24) mean that the reduction in the maximum stress and deflection depends on the scaling factor p_y along the *y*-axis and is independent of the scaling factor p_x along the *x*-axis. This means that if the scaling factor along the *y*-axis is $p_y = 1$, then $\sigma_{t,1} / \sigma_{t,2} = 1$ and $\delta_1 / \delta_2 = 1$, and although $p_x > 1$, the aggregation into fewer load-carrying elements with larger cross sections will not entail any stress and deflection reduction.

A further increase in the load-bearing capacity could be achieved by tapering the cantilevered beam. This is a textbook approach to enhancing load-bearing capacity by increasing thickness at the fixed end and gradually decreasing it towards the free end. For a given total material volume, this tapered shape improves load-bearing efficiency. However, for the sake of simplicity in presenting the underlying theory, a uniform cross-section along the beam's length is intentionally chosen to simplify the theoretical exposition of the aggregation method.

This choice in no way diminishes the advantages of the proposed method. As can be verified from **Fig.2**, even with a uniform cross-section, the material savings required to support the same total load are very large. For example, with a five-to-one aggregation, material usage is reduced by a factor of 1.71.

Aggregation must be applied judiciously, considering structural redundancy and operational conditions. For example, if a structure with four supporting elements must remain functional after the failure of any element, a 4-to-2 aggregation may be unsuitable. However, by no means does aggregation promote structural collapse. In fact, an aggregated structure exhibits significantly increased load-bearing capacity and a much larger margin of safety than its non-aggregated counterpart.

A possible implementation challenge of the method of aggregation is the unavailability of standard elements with cross-sections with scaling factor p_y along the y-axis greater than 1. It must be pointed out that theorems 1 and 2 have been proved for cross sections that are not necessarily geometrically similar because $p_x \neq p_y$.

4. Testing the aggregation method using finite element analysis

The method of aggregation was tested on structures composed of statically determinate cantilevered structures and statically indeterminate Π-frames. The verification of the aggregation method was conducted using steel components made of high carbon steel, heat treated to create a strong elastic material with Young's modulus of 200 GPa and a Poisson's ratio of 0.3. The steel components have been subjected to 8-to-2 aggregation. The maximum von Mises stress and the maximum deflections have been analyzed using the finite element analysis software Abaqus/CAE 2021.

4.1 Testing the aggregation method on cantilevered beams

One of the ends of the statically determinate cantilevered beam is fixed, while the other end is free (**Fig.3a** and **3b**). The distance between the fixed support and the end of the beams is L = 100 mm for both the non-aggregated (**Fig.3a**) and aggregated beams (**Fig.3b**).

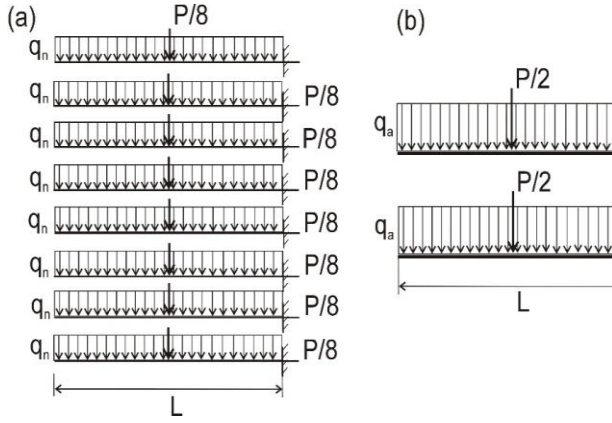

Fig.3. Testing the aggregation method on statically determinate cantilevered I-beams.

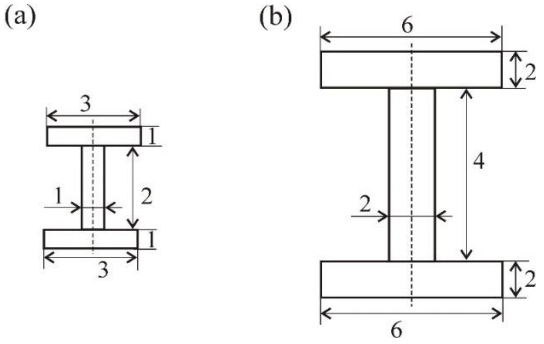

Fig.4. Cross sections of the (a) non-aggregated and (b) aggregated I-beams. All dimensions are in millimeters.

The cross sections of the non-aggregated and aggregated beams are according to **Fig.4a** and **4b**, respectively. The dimensions of the cross-sections have been selected such that the total volume of material in eight non-aggregated beams (**Fig.3a**) is exactly equal to the total volume of material in two aggregated beams (**Fig.3b**).

The same total load P=360N has been applied to both the aggregated and non-aggregated structure. As a result, each beam from the non-aggregated structure in **Fig.4a** (8 beams) is loaded with a force of 360/8=45N, distributed uniformly along the top surface of the beam. Each beam of the aggregated structure (2 beams) is loaded with a force of 360/2=180N (8×45N = 2×180N=360N), distributed uniformly along the top surface of the beam. The global size of the selected hexahedral mesh for the non-aggregated beams was 0.0001mm while for the aggregated beams, the mesh size was 0.0002mm. The boundary condition of the fixed end was of the type ENCASTRE.

Table 1 lists the maximum von Mises stress and the maximum deflection characterizing non-aggregated and aggregated cantilever beams. From the table, it can be concluded that for the same total applied load (360 N), the aggregated structure experiences significantly lower maximum von Mises stress and maximum deflection compared to the non-aggregated structure. The ratio of the maximum von Mises stresses of the non-aggregated and aggregated structures is 350/179 = 1.95, which is close to the scaling factor $p_y = 2$ along the y-axis. The ratio of the deflections of the non-aggregated and aggregated structures is 1.92/0.48 = 4, which is equal to the square of the scaling factor along the y-axis $p_y^2 = 4$. These values correlate well with the theoretical predictions regarding the maximum tensile stress and maximum deflection for cantilever beams. The deviation of the ratio of stresses from $p_y = 2$ is present because von Mises stresses were calculated in the finite element analysis rather than the maximum tensile stress.

Table 1. Finite element analysis results for the maximum von Mises stress and deflection of non-aggregated and aggregated statically determinate cantilever beams.

	Non-aggregated	**Aggregated**
Maximum von Mises stress	350 MPa	179 MPa
Maximum deflection	1.92 mm	0.48 mm

4.2 Testing the aggregation technique on statically indeterminate Π-frames

Testing of the aggregation technique was also conducted on centrally loaded and side loaded statically indeterminate portal frames (Π-frames). The aggregation selected for the Π-frames was 8 to 2. Eight centrally loaded frames (**Fig.5a**) with square cross sections with side 1mm are aggregated into two centrally loaded portal frames (**Fig.5b**) with a square cross-section with side 2 mm). **Fig. 5** shows the dimensions of the Π-frames in mm. Because the length of the frames is the same, the same total volume of material characterizes both structures. Both structures are also subjected to the same total loading force of P=160 N. This means that the load applied on an individual non-aggregated Π-frame is 160/8=20 N, uniformly distributed over the top surface of the non-aggregated frame (**Fig.5a**).

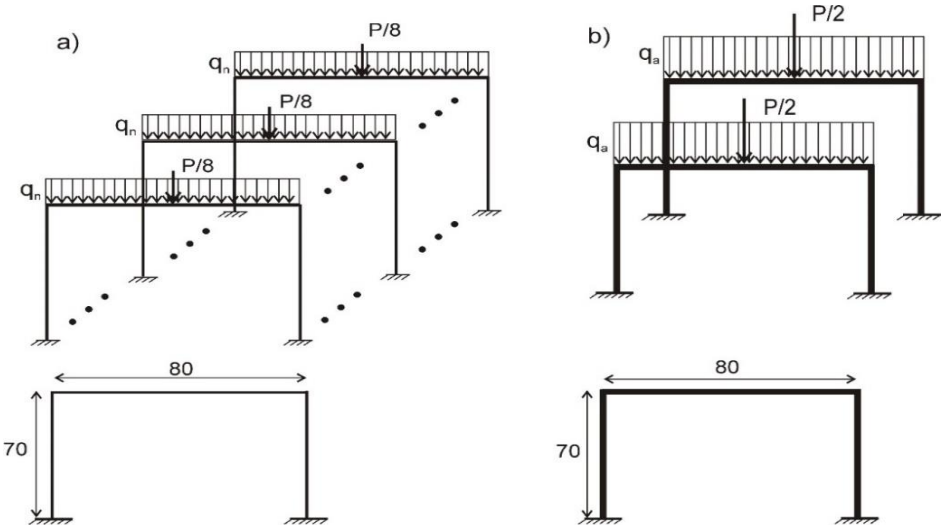

Fig.5. Eight-to-two aggregation of centrally-loaded portal frames (Π-frames). Dimensions are in millimeters.

The load applied on an individual aggregated Π-frame is 160/2=80N, uniformly distributed over the top surface of the aggregated frames in **Fig.5b**. The Young's modulus of the material for all Π-frames is 200 GPa and the Poisson's ratio is 0.3.

The maximum von Mises stresses and deflections of the Π-frames were determined by using finite element analysis in Abaqus/CAE 2021. The global size of the selected hexahedral mesh was 0.0001mm for the non-aggregated frames and 0.0002 mm for the aggregated frames. The boundary conditions of the fixed ends of the frames were of the type ENCASTRE.

Table 2 lists the maximum von Mises stresses and deflections. The analysis of the results in Table 2, for centrally loaded Π-frames, shows that aggregated frames experience significantly smaller maximum von Mises stresses and deflections compared to non-aggregated frames.

Table 2. Results for the maximum von Mises stress and maximum deflection for centrally-loaded non-aggregated and aggregated Π-frames.

	Non-aggregated	**Aggregated**
Maximum von Mises stress	570.7 MPa	302.3 MPa
Maximum deflection	3.39 mm	0.8 mm

The ratio of the maximum von Mises stresses of the non-aggregated and aggregated structures is 570.7/302.3 = 1.89 while the ratio of the deflections of the non-aggregated and aggregated structures is 3.39/0.8 = 4.24. **Fig. 6** gives a contour plot (exaggerated) of the deflections of the centrally loaded, aggregated Π-frame.

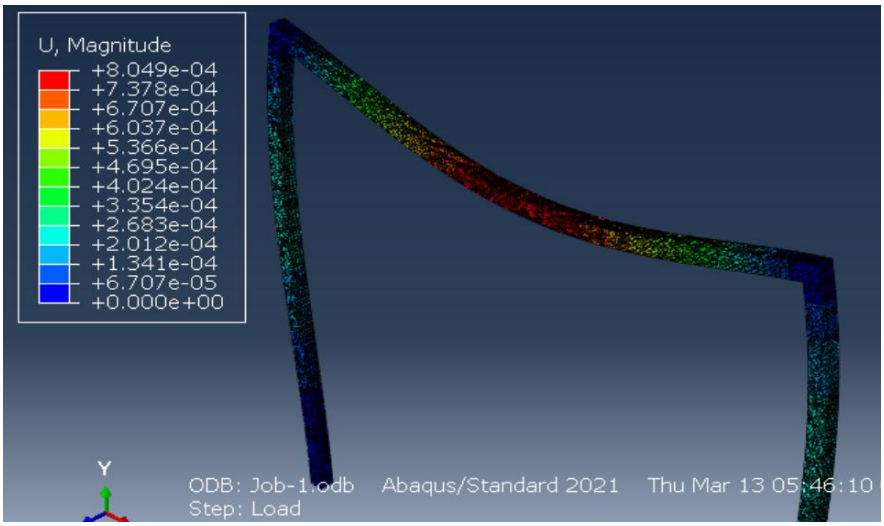

Fig.6. Deflections of the centrally-loaded, aggregated Π-frame obtained by Abaqus/Standard 2021.

Testing of the aggregation method was also conducted on a side-loaded statically indeterminate Π-frames. The aggregation selected for the side-loaded Π-frames was also 8 to 2. (eight loaded frames (**Fig.7a**) with square cross sections with side 1mm are aggregated into two side-loaded frames (**Fig.7b**) with a square cross-section with side 2 mm). **Fig. 7** gives the dimensions of the side loaded Π-frames (in mm). Both structures were subjected to the same total loading force of $P = 56\text{N}$. The load applied on an individual non-aggregated Π-frame is 56/8=7 N, uniformly distributed over the surface of the vertical section of the non-aggregated frame (**Fig.7a**).

The load applied on an individual aggregated Π-frame is 56/2=28N, uniformly distributed over the right vertical section of the aggregated frame (**Fig.7b**). The Young's modulus of the material for all side-loaded Π-frames is 200 GPa and the Poisson's ratio is 0.3.

The maximum von Mises stresses and deflections of the side-loaded Π-frames were also determined by using finite element analysis in Abaqus/CAE 2021. The global size of the hexahedral mesh was 0.0001mm for the non-aggregated frames and 0.0002mm for the aggregated frames. The boundary conditions of the fixed ends of the frames were of the type ENCASTRE. **Fig. 8** gives a contour plot (exaggerated) of the deflections of the side-loaded, aggregated Π-frame.

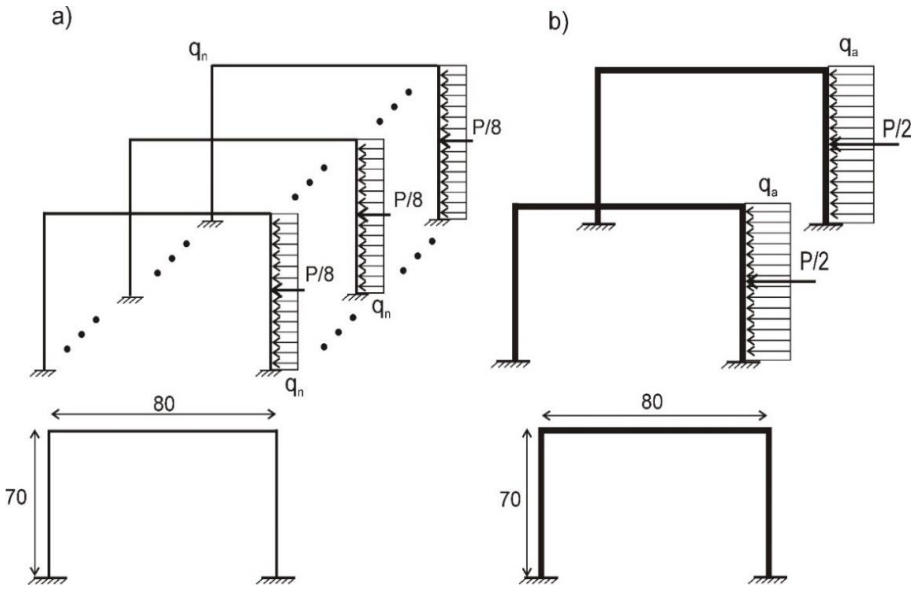

Fig.7. Eight-to-two aggregation of side-loaded portal frames (Π -frames). Dimensions are in millimeters.

The results related to the maximum von Mises stresses and deflections are listed in Table 3. The analysis of the results in Table 3 for side-loaded Π -frames shows that the aggregated frames also experience significantly smaller von Mises stresses and deflections compared to non-aggregated frames.

Table 3. Results for the maximum von Mises stress and maximum deflection for side-loaded non-aggregated and aggregated Π -frames.

	Non-aggregated	**Aggregated**
Maximum von Mises stress	634.5 MPa	315.4 MPa
Maximum deflection	3.94 mm	0.97 mm

The ratio of the maximum von Mises stresses of the non-aggregated and aggregated frames is 634.5/315.4 = 2.01 while the ratio of the deflections of the non-aggregated and aggregated frames is 3.94/0.97 = 4.06. Figure 8 gives a contour plot (exaggerated) of the deflections of the side-loaded Π -frame.

The simulation studies demonstrated that, similar to statically determinate structures, aggregation also had a dramatic effect on the maximum von Mises stress and the maximum deflection of statically indeterminate frames.

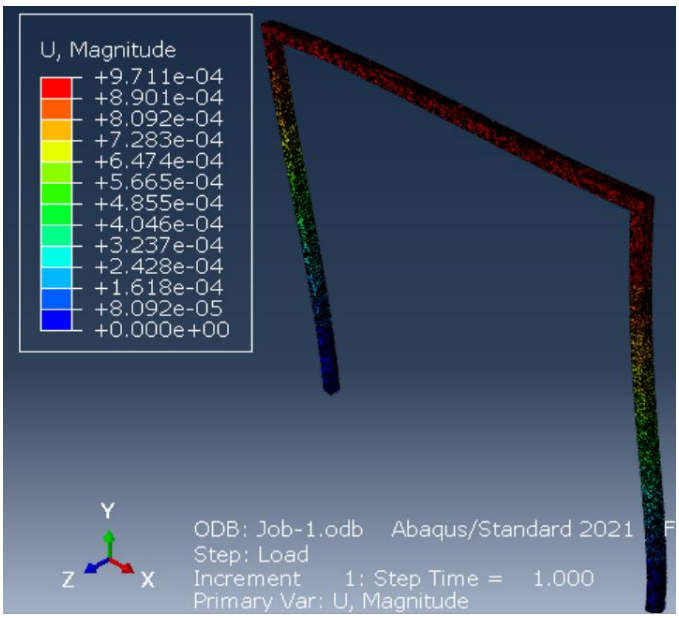

Fig.8. Deflections of the side-loaded, aggregated Π -frame obtained by Abaqus/Standard 2021

5. Conclusions

Aggregating beams with arbitrary cross-sectional shapes into fewer beams with larger cross sections leads to a dramatic decrease in the volume of material required to support a specified total load. For example, in the case of five-to-one aggregation of cantilever and simply supported beams, the total volume of material needed to support the same load is reduced by a factor of 1.71.

A theorem has been stated and proved that provides the foundation for the aggregation method used to reduce the volume of material in structures composed of beams with arbitrary cross sections. For a specified total load, the ratio of the minimum necessary volumes of material for the non-aggregated and aggregated structures is determined by the scaling factor of the aggregated section along the *y*-axis. The ratio of the deflections is also given by this same scaling factor. These results hold regardless of the shape of the cross-sectional area of the loaded beams.

A case study involving I-beams confirmed the key theoretical findings and demonstrated the significant impact that aggregation has on the minimum amount of material necessary to carry a specified load.

A theorem has also been proven that provides the foundation for the aggregation method in structures under the same total load, containing the same total volume of material. For an equal total volume of material, the ratio of the maximum tensile stresses in the non-aggregated and aggregated structure is equal to the scaling factor of the aggregated section along the *y*-axis, while the ratio of the maximum deflections is given by the square of this scaling factor. These results hold regardless of the shape of the cross sections of the loaded beams.

The reduction in material volume, deflection, and stress depends solely on the scaling factor of the cross section along the *y*-axis and is independent of the scaling factor along the *x*-axis. This means that if the scaling factor along the *y*-axis is unity, aggregation into fewer load-carrying elements with larger cross sections will not result in any reduction in volume, deflection, or stress.

The aggregation method was tested through finite element experiments, which confirmed that aggregating statically determinate cantilever beams and statically indeterminate frames, under the same total load, leads to a drastic decrease in both the maximum von Mises stress and the maximum deflection.

Further Work

The aggregation method can be further developed by:

- Developing the method for an inhomogeneous scaling factor p_y along the *y*-axis. (i.e. different parts of the cross-section are scaled by with different factors p_y.
- Testing the aggregation method on complex structural systems and structures composed of elements made from different materials.
- Testing the aggregation method on physical prototypes.

Funding Statement

The author received no specific funding for this study.

Conflicts of Interest

The author declares that he has no conflicts of interest regarding the present study.

Data Availability Statement

All data and models that support the findings of this study are available from the author upon reasonable request.

References

[1] Todinov M. Mechanisms for improving reliability and reducing risk by stochastic and deterministic separation, Journal of Risk Research, 2019; 22(4): 448-474, DOI:10.1080/13669877.2017.1382561.

[2] Zhu, J., Zhou, H., Wang, C., Zhou, L., Yuan, S. and Zhang, W. A review of topology optimization for additive manufacturing: Status and challenges, Chinese Journal of Aeronautics, 2021; 34(1): 91-110: https://doi.org/10.1016/j.cja.2020.09.020.
[3] Walton, D.; Moztarzadeh, H. Design and Development of an Additive Manufactured Component by Topology Optimization. Procedia CIRP 60, 205–210. Chinese Journal of Aeronautics 2017; 33(12): 3206-3219: https://doi.org/10.1016/j.procir.2017.03.027.
[4] Zhao Z., Kang Z., Zhang T., Zhao B., Zhang D., Yan R. Topology optimization algorithm for spatial truss based on numerical inverse hanging method, Journal of Constructional Steel Research, 2024; 219: 108764. https://doi.org/10.1016/j.jcsr.2024.108764.
[5] Bikas H., Stavropoulos P. and Chryssolouris1 G. Additive manufacturing methods and modelling approaches: a critical review, International Journal of Additive Manufacturing Technology 2016; 83:389–405. DOI 10.1007/s00170-015-7576-2.
[6] Yang L., Harrysson O.L.A., Cormier D., West H., Zhang S., Gong H., Stucker B. Design for Additively Manufactured Lightweight Structure: A Perspective, Solid Freeform Fabrication, Proceedings of the 26th Annual International Solid Freeform Fabrication Symposium – An Additive Manufacturing Conference 2016.
[7] Mandolini, Pradel P. and Cicconi P.. Design for Additive Manufacturing: Methods and Tools, Appl. Sci. 2022; 12(13): 6548, MDPI: https://doi.org/10.3390/app12136548.
[8] Rosenthal, S. Maaß, F., Kamaliev, M., Hahn, M., Gies, S., Tekkaya, A.E. Lightweight in automotive components by forming technology. Automot. Innov. 2020; 3: 195–209: https://doi.org/10.1007/s42154-020-00103-3.
[9] Buragohain M.K. Composite Structures: Design, Mechanics, Analysis, Manufacturing, and Testing, CRC Press: 2017; https://doi.org/10.1201/9781315268057.
[10] Beer F.P., Russell Johnston E. Jr, DeWolf J.T. Mechanics of Materials, 3rd ed. McGrawHill, New York, 2002; ISBN-13 978-0073380285.
[11] Gere J.M. and Timoshenko S.P. Mechanics of Materials, 4th SI edition, Stanley Thornes (Publishers) Ltd. 1999; ISBN-13: 978-0748739981.
[12] Zhou Y., Uy B.,Wang J., Dongxu Li D. Behavior and design of welded stainless steel beams with compact sections under flexure and shear, Journal of Constructional Steel Research, 2021; 187: 106996: https://doi.org/10.1016/j.jcsr.2021.106996.
[13] Su Q., Fu G., Yang J., Li S. (2025). Experiment and numerical analysis of prestressed unequal-walled rectangular concrete-filled steel box beams, Nature portfolio, Scientific Reports volume 15, 2025; Article number: 425. https://doi.org/10.1038/s41598-024-84473-2.
[14] Budynas R.G. 1999. Advanced strength and applied stress analysis. 2nd ed. New York: McGraw-Hill 1999; ISBN-13: 978-0070089853.
[15] Budynas, R. G., & Nisbett, J. K. Shigley's Mechanical engineering design (10th ed.). McGraw-Hill Education 2015; ISBN-13: 978-0073398204.
[16] Collins, J. A. Mechanical design of machine elements and machines. New York: John Wiley & Sons, Inc. 2015; ISBN-13: 978-0471033073.
[17] Hearn E.J. Mechanics of materials. 2nd ed. Oxford: Butterworth-Heinemann, 1985; vol.1: ISBN-13: 978-0080311319.
[18] Hibbeler R.C. Statics and Mechanics of Materials, SI edition, Pearson 2004; ISBN-13: 978-9814526043.
[19] Hibbeler, R.C. Structural Analysis, 10th SI Edition, Pearson, 2019; ISBN-13: 978-1292247137.
[20] Williams A. Structural Analysis in theory and practice, 1st Edition - December 12, 2008, Butterworth-Heinemann: 2008; ISBN-13: 978-1856175500.
[21] Podder D., Chatterjee S. An introduction to structural Analysis, CRC press, 2022; ISBN-13: 978-0367532734.
[22] Yanga K-H, Ashourb A.F. Aggregate interlock in lightweight concrete continuous deep beams, Engineering Structures, 2011; 33:136–145: http://hdl.handle.net/10454/7562.
[23] Qiao H. and Li H. The discussion on optimization models of pure bending beam, International Journal of Advanced Structural Engineering, 2013; 5:11: https://doi.org/10.1186/2008-6695-5-11.
[24] Wang C. Structural Reliability and Time-Dependent Reliability, Springer Series in Reliability Engineering, 2020; ISBN-13: 978-3030625047.
[25] Kiureghian A. Structural and System Reliability, Cambridge University Press. Long CHEN, Yanlai ZHANG, Zuyong CHEN, Jun XU, Jianghao Wu. Topology optimization in lightweight design of a 3D-printed flapping-wing micro aerial vehicle: 2022; ISBN-13 978-1108834148.

Appendix. A case study related to reducing the volume of material for supporting console arms with arbitrary shape of the cross-section

Consider the four steel console arms in Fig.A1a with an arbitrary shape of the cross-section according to Fig.A2a and length L=1.5m, supporting a total weight of P=9000N. A conservative assumption has been made that the total load of P=9000N is concentrated at the free end of the supporting console arms. For the sake of simplicity, it is also assumed that the total load P is distributed uniformly across the supporting console arms, and each console arm supports a quarter (P/4) of the total load P (see Fig.A1a).

If the four supporting console arms from Fig.A1a are aggregated into two supporting console arms (Fig.A1b), an aggregation 4-to-2 will be made. The aggregated structure in Fig.A1b consists of two steel console arms with cross-sectional area according to Fig.A2b and the same length of L=1.5m. The aggregated structure carries the same total load of 9000N. Similar to the non-aggregated structure, it is assumed that the total weight P is distributed uniformly across the two aggregated console arms, and each console arm supports a half of the total weight (P/2; see Fig.A1b). The Young's modulus of the material of all I-beams is 200GPa.

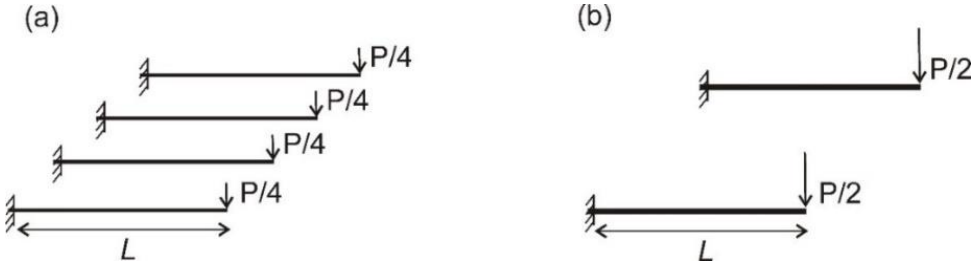

Fig. A1. (a) Non-aggregated supporting structure built on four I-beams (b) Aggregated supporting structure built on two I-beams.

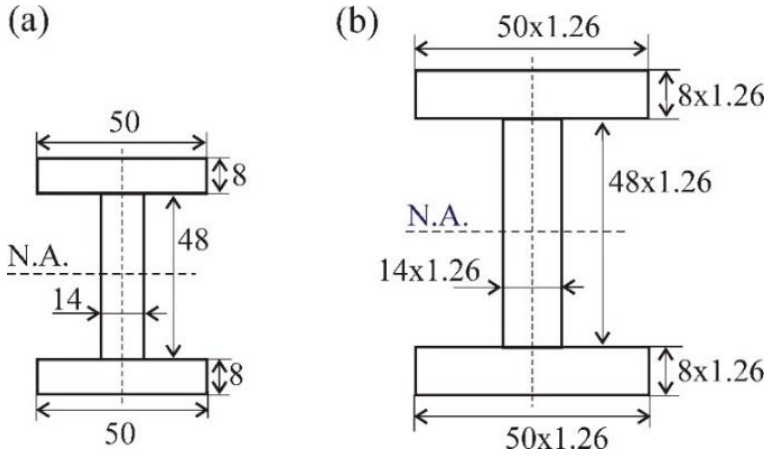

Figure A2. Cross-sections of the (a) non-aggregated and (b) aggregated supporting elements. Dimensions are in millimeters.

The cross-sections in Fig.A2a and A2b have been assumed to be geometrically similar which means that the scaling factors p_x, p_y along both axes are equal ($p_x = p_y = p$). To ensure equal maximum tensile stress in both non-aggregated and aggregated beams, the scaling factors are determined using Equation (15):

$$p_x = p_y = p = (n/m)^{1/3} = (4/2)^{1/3} = 1.26$$

The dimensions of the cross sections of the aggregated console arms are according to Fig.A2b. They are proportional to the dimensions of the non-aggregated structure (Fig.A2a) with a proportionality factor equal to 1.26.

Maximum tensile stress and maximum deflection of the non-aggregated and aggregated structures

The cross-section in Fig.A2a is symmetrical, with a neutral axis denoted by N.A. passing through the centroid of the cross section. Applying the parallel-axis theorem gives the following value for the second moment of area I_a of the cross section in Fig.A2a:

$$I_{\mathrm{a}} = 2\times\left(50\times 8^3/12 + 50\times 8\times 28^2\right) + 14\times 48^3/12 = 760.49\times 10^{-9} \quad m^4$$

For the maximum tensile stress at the fixed support of the console arm, the value:

$$\sigma_{\mathrm{t,a}} = \frac{(P/4)L}{I_{\mathrm{a}}}\hat{y}_{\mathrm{a}} = \frac{(9000/4)\times 1.5}{760.49\times 10^{-9}}\times 32\times 10^{-3} = 142MPa$$

is obtained, where $\hat{y}_a$ is the largest distance from the neutral axis for the section in Fig.A2a.

The maximum deflection of the non-aggregated console arms under the action of a concentrated force P/4 of magnitude 9000/4 N is calculated using a well-known dependence from the simple bending theory:

$$\delta_{\mathrm{a}} = \frac{(P/4)L^3}{3EI_{\mathrm{a}}} = \frac{(9000/4)\times 1.5^3}{3\times 200\times 10^9\times 760.49\times 10^{-9}} = 0.0166m\,(16.6mm)$$

Similarly, the second moment of area of the cross section in Fig.A2b, determined by applying the parallel axis theorem is:

$$I_{\mathrm{b}} = 2\times\left(50\times 1.26\times(8\times 1.26)^3/12 + 50\times 1.26\times 8\times 1.26\times(28\times 1.26)^2\right) +$$
$$14\times 1.26\times(48\times 1.26)^3/12 = (1.26)^4 I_a = 1916.8\times 10^{-9}\ m^4$$

The maximum tensile stress at the fixed support of the aggregated console arm is:

$$\sigma_{\mathrm{t,b}} = \frac{(P/2)L}{I_{\mathrm{b}}}\hat{y}_{\mathrm{b}} = \frac{(9000/2)\times 1.5}{1916.8\times 10^{-9}}\times 32\times 1.26\times 10^{-3} = 142MPa$$

while the maximum deflection of the aggregated console arms is:

$$\delta_{\mathrm{b}} = \frac{(P/2)L^3}{3EI_{\mathrm{b}}} = \frac{(9000/2)\times 1.5^3}{3\times 200\times 10^9\times 1916.8\times 10^{-9}} = 0.0132m\ (13.2\,mm)$$

where $\hat{y}_{\mathrm{b}}$ is the largest distance from the neutral axis for the section in Fig.A2b.

As can be verified from the calculations, after the aggregation, the maximum tensile stress remained the same as in the non-aggregated structures, but the maximum deflection has been reduced significantly (by a factor of 1.26). At the same time, the total volume of material needed to support a total load of 9000N has also been decreased 1.26 times.

Indeed, for the ratio of the maximum deflections, we have: $\delta_a/\delta_b = 16.6/13.2 = 1.26$. Next, the volume $V_{\mathrm{a,1}}$ of a single non-aggregated console arm, with a cross-section according to Fig.2a, is given by

$$V_{\mathrm{a,1}} = [2\times 50\times 8 + 14\times 48]\times 1500 = 2208\times 10^3 mm^3$$

The volume $V_{\mathrm{b,1}}$ of a single aggregated console arm, with a cross-section according to Fig.A2b, is given by

$$V_{b,1} = [2\times 50\times 1.26\times 8\times 1.26 + 14\times 1.26\times 48\times 1.26]\times 1500 = (1.26)^2 V_{a,1}$$
$$= 3505.42\times 10^3 mm^3$$

For the total volume $V_{a,total}$ of 4 non-aggregated console arms in the structure from Fig.A1a, we have:

$$V_{a,total} = 4\times V_{a,1} = 8832\times 10^3 mm^3$$

and for the total volume $V_{b,total}$ of 2 aggregated console arms in the structure from Fig.A1b, the result is

$$V_{b,total} = 2\times V_{b,1} = 2\times 3505.42\times 10^3 = 7010.84\times 10^3 mm^3$$

The ratio of the volumes of material for the non-aggregated and aggregated structures is given by

$$V_{a,total} / V_{b,total} = 8832\times 10^3 / 7010.84\times 10^3 = 1.26 .$$

These results agree with the predictions from the theory presented in Section 2. The aggregated structure has the same maximum permissible stress as the non-aggregated structure but a significantly smaller total volume of material and a significantly smaller maximum deflection.